

## FLEXURAL PROPERTIES OF OIL PALM WOOD (*ELAEIS GUINEENSIS* JACQ.) BASED GLUED LAMINATED TIMBER (GLT) USING FINITE ELEMENT METHOD (FEM)

Martin Hackel<sup>1</sup>

**ABSTRACT:** The anatomical structure of oil palm wood is only to a limited extent comparable to common wood species used in construction. Typical for monocotyledons, the material is composed of high density vascular bundles and a parenchymatous tissue of lower density. In three experiment sets, the local and global moduli of elasticity (MOE) and the flexural strength of oil palm wood based GLT are determined using FEM and various influencing parameters are investigated in a sensitivity analysis. Furthermore, the application of densified tension lamellas is studied. The results of the modelling are compared with the results from mechanical tests. Significant differences, mainly attributed to the specific parameters of the selected material, are observed. The results of this preliminary study serve as a starting point for computer-aided optimisation and modelling of other oil palm-based products.

**KEYWORDS:** Oil palm wood, finite element method (FEM), GLT, modulus of elasticity, flexural strength

### 1 INTRODUCTION

The rising population in recent decades has led to increased demand for raw materials, especially in the food, chemical and pharmaceutical industries as well as the construction and energy sectors. Oil palms (*Elaeis guineensis* JACQ.) are a versatile raw material producing crop. Oil palm provides raw materials in the form of palm and palm kernel oil, for all industry sectors mentioned. As a result, the global oil palm cultivation area, concentrated in Southeast Asia, increased between 1996 and 2021 by 328 % to 28.9 million hectares [1]. Declining crop yields limit the economic lifespan of oil palms to about 25 to 30 years [2]. The clearing of plantation areas after the end of the economic lifespan results in up to 180 million m<sup>3</sup> of usable oil palm wood per year [3]. Its actual use, however, is limited by a lack of knowledge regarding the wood's material properties. Possible substitution potentials of the material are also unrecognised and accordingly not utilised. Influenced by the shortage of building products caused by various factors, such as the conflict in Ukraine, droughts and bark beetle calamities in Europe and North America as well as the effects of the Covid pandemic, building products have been identified as a possible field for substitution approaches.

The development of construction materials from renewable raw materials (e. g. wood or wood like materials) is economically intensive. These raw materials are characterized by inherent variations of their material properties and naturally occurring inhomogeneity. Common building materials such as glued laminated timber (GLT) use layer-based approaches to reduce the property variations respectively the inhomogeneity. The application, production and properties of GLT are specified by e.g. European standards [4, 5]. Before oil

palm based GLT can be introduced to the market, it is necessary to create a lamella grading [6] and develop various beam structures in regard to the requirements in the standards. Therefore, expensive material tests need to be performed. A way to reduce costs is through digitalisation. Larger series of experiments can be performed using the finite element method (FEM) without material expense and in a comparatively short investigation period. The quality of FEM-modelling depends on the quality of the material parameters used as input parameters. But suitable material parameters of oil palm wood are only published to a limited extent in the literature. Currently, no modelling of oil palm wood based products has been published.

The aim of the work is to evaluate the suitability of FEM for determining the flexural properties of oil palm GLT by comparing the modelling results with the results of Heister and Fruehwald-Koenig [7] (static tests). Furthermore, possible relationships of the flexural properties with other material properties, primarily density, are evaluated. In the form of a sensitivity analysis, possible influences of different material properties on the flexural strength are examined. Furthermore, the influence of densified tension lamellas on the flexural strength is evaluated.

The objectives of the work are achieved through a multi-stage process. Based on a literature research, suitable relationships between the density and elastomechanical material properties are determined. Missing relationships are established by own investigations or approximation. The beams tested by Heister and Fruehwald-Koenig [7] are implemented in the modelling software RFEM 6.02. Using suitable statistical methods, the results of the different experiments are compared and evaluated.

<sup>1</sup> Martin Hackel, OWL University of Applied Sciences and Arts, Lemgo, Germany, martin.hackel@th-owl.de

Subsequently, correlations of the modelling results with different specimen properties are investigated. Following this, the results of the modelling are compared with the results of the experiments by Heister and Fruehwald-Koenig [7]. Finally, the results are discussed and placed in the context of existing literature.

## 2 STATE OF THE ART

### 2.1 ANATOMICAL FEATURES OF OIL PALM WOOD

Oil palms (*Elaeis guineensis* JACQ.) are monocotyledons and show differences in the anatomical structure to dicotyledons (deciduous and coniferous trees). Monocotyledons have no cambium, which results in a lack of annual rings (no secondary thickness growth). Furthermore, oil palms have no wood rays, no differentiation between heartwood and sapwood and no knots. Oil palm wood is composed of vascular bundles of high density and parenchymatous ground tissue of low density. The vascular bundles are mainly parallel to the mantle, but also helical orientations are widespread [8]. Deviations from the stem axis occur due to direct contact with the palm fronds and are therefore also referred to as leaf trace bundle [9].

Lim and Khoo [2] define three zones within the oil palm stem. The “outer” or “peripheral” zone of the stem includes about 20 % of the stem volume, irregular vascular bundles and a low parenchyma content characterise this zone [10]. The “inner” zone (about 40 % of the stem volume) has a high parenchyma content and widely distributed vascular bundles. The “central” zone (approx. 40 % stem volume) forms a transition between the peripheral and inner zone. Lim and Khoo [2] report densities of 170 kg/m<sup>3</sup> from the “inner” zone to 700 kg/m<sup>3</sup> in the “outer” zone. Kölli [11] confirms this density range (180 kg/m<sup>3</sup> - 561 kg/m<sup>3</sup>). With increasing trunk height, the density of oil palm wood decreases. Kölli [11] shows exponential relationships between the position in the trunk and the density (horizontal and vertical). The “wood” tissue of oil palms is anisotropic, but only small property differences between radial and tangential directions are reported [2, 10]. Nevertheless, orthotropic material behaviour is assumed in the context of this work.

### 2.2 ELASTOMECHANICAL PROPERTIES OF OIL PALM WOOD

In compression tests (longitudinal), Fathi [12] determines Young's moduli of 1856 to 8238 MPa with a linear relationship ( $R^2 = 0.99$ ) to the density. Srivaro et al. [13] determine values for the Young's modulus (longitudinal) of 114 to 996 MPa and an exponential relationship with the density ( $R^2 = 0.64$ , exponent 2.67). In the tensile test in fibre direction, Fruehwald-Koenig and Heister [14] determine a Young's modulus of 488 to 13102 MPa and report an exponential relationship to the density ( $R^2 = 0.53$ , exponent 2.41). A determination of the Young's modulus along all anatomical axes is performed by Fruehwald-Koenig and Faust [15] using ultrasonic measurements. Values of 4368 to 11695 MPa and a linear correlation with the density ( $R^2 = 0.75$ ) are determined for the longitudinal Young's modulus. The values of the

radial Young's modulus range from 100 to 501 MPa. The correlation to the density is low ( $R^2 = 0.04$ ). The tangential Young's modulus is determined with values from 91 to 743 MPa and a linear relationship with density is shown ( $R^2 = 0.26$ ).

$G_{TL}$  and  $G_{RL}$ , respectively, are determined by Koelli [16] in static shear tests. The reported relationships are determined using linear or exponential regression models and provide coefficients of determination of  $R^2 = 0.39$  (linear) or  $R^2 = 0.43$  (exponential). Fruehwald-Koenig and Faust [15] determine the G-moduli in all three planes by dynamic ultrasound measurements. The results for  $G_{LR}$  range from 189 to 472 MPa, for  $G_{TL}$  from 196 to 555 MPa and for  $G_{RT}$  from 167 to 345 MPa. For all G-moduli, linear relationships with density are evident ( $R^2 = 0.69 - 0.85$ ). The Poisson's constants are determined by Fruehwald-Koenig and Faust [15] by dynamic ultrasonic measurements. The mean values of the individual constants are given as follows:  $\mu_{LR} = 0.389$ ,  $\mu_{RL} = 0.026$ ,  $\mu_{LT} = 0.911$ ,  $\mu_{TL} = 0.044$ ,  $\mu_{RT} = 0.647$  and  $\mu_{TR} = 0.707$ . Fruehwald-Koenig et al. [17] determine Poisson's constants on specimens in service dimensions. The measurements do not distinguish between radial and tangential directions. Mean values for  $\mu_{L/RT}$  from 0.379 to 0.523 and  $\mu_{RT}$  of 0.117 are reported. Relationships between density and Poisson's constants are not pronounced ( $R^2 = 0.0024$ ).

For oil palm wood, no data on hardening moduli are available at the time of writing. Fruehwald-Koenig and Heister [14] determine the tensile strength (longitudinal) with values from 1.9 to 47 MPa and show an exponential relationship to the density ( $R^2 = 0.76$ , exponent 2.24). Furthermore, tensile strength (radial/tangential) with values of 0.4 to 2.3 MPa and an exponential relationship ( $R^2 = 0.5$ , exponent 1.4) are reported.

Fathi [12] determines compressive strengths (longitudinal) with values from 4.4 to 27.6 MPa and shows a linear relationship with density ( $R^2 = 0.6$ ). Fruehwald-Koenig and Heister [14] demonstrate an exponential relationship ( $R^2 = 0.76$ , exponent 2.24) and reported values from 3.1 to 64.6 MPa. For the compressive strength (radial/tangential) an exponential relationship ( $R^2 = 0.73$ , exponent 3.08) and values from 0.1 to 12.2 MPa are reported.

Investigations by Fathi [12] regarding the shear strength in RL-plane with longitudinal load provide results of approximately 2 to 4 MPa and a linear relationship with density ( $R^2 = 0.998$ ). Fruehwald-Koenig et al. [17] determine an exponential relationship with density ( $R^2 = 0.52$ , exponent 1.36) for the shear strength in RL plane under longitudinal load and report values from 0.2 to 7.8 MPa. In addition, rolling shear strengths with values from 0.1 to 3.1 MPa and a moderate exponential relationship with density ( $R^2 = 0.17$ , exponent 1.05) are determined.

### 2.3 FEM FOR LAYER BASED WOODEN PRODUCTS

FEM is used to model the material behaviour of GLT beams and other layer-based wooden materials. Ehlbeck et al. [18] use FEM to predict the load-bearing capacity of glulam beams made of spruce. The material behaviour is assumed to be linearly elastic. The load is increased

stepwise. Within each stage, all elements are tested against reaching the tensile or compressive strength. When the tensile strength is reached, a case distinction is made. If the applied load is greater than in the previous load level, the material properties of the element are set to zero and the load is increased further. If the load is less than in the previous load level, the load-bearing capacity is reached. When the compressive strength is reached, the properties of the element are changed so that no further load absorption is possible [18]. Blaß et al. [19] and Frese [20] transfer the approach of Ehlbeck et al. [18] to beech wood. Orthotropic linear elastic material behaviour is assigned to the tension zone. The failure of the beam is defined by reaching the tensile strength in one element of the tension lamella. The elements of the compression zone are assigned an ideal elastic-plastic material model [19–20]. If the compressive strength is exceeded, ideal plastic material behaviour is assumed. The deviations between modelling and laboratory tests are between -6.9 % and +2.5 % (flexural strength) and -8.1 % and +1.9 % (global MOE) [20]. Gao et al. [21] transfer the aforementioned approach to Cathay poplar. Deviating from Blaß et al. [19], a three-dimensional model and steel intermediate layers (riders) are used in the load application points. In addition, the adhesive bond is investigated. Isotropic material properties are assigned to the adhesive layers. The bond between adhesive and timber layers is assumed to be rigid. The assignment of the material models in tension and compression zone is realised analogous to Frese [20]. Modelling underestimates the flexural strength by 3.9 % and overestimates the global MOE by 2.8 %.

### 3 MATERIAL

#### 3.1 MATERIAL ORIGIN

The material used in the laboratory tests [7] originates from two cultivation regions in Malaysia. The material of the specimens with the identifiers ZA and ZN is obtained from approximately 30-year-old oil palms from the Kedah region. The material is transported to Germany in frozen state. Further processing takes place in Germany. Information on processing and drying can be found in Heister and Fruehwald-Koenig [7]. The material of specimen identifiers A and N originates from the Johor region. The cutting of the palms (approximately 30 years old) as well as the drying are carried out within the framework of a research project of the Forest Research Institute of Malaysia (FRIM). Further information on the processing of the material is provided by Heister and Fruehwald-Koenig [7].

#### 3.2 BEAM STRUCTURES

Within the scope of this work, combined GLT beams are investigated. The beams have the dimension 2200 mm x 50 mm x 102 mm and consist of six lamellas each (2200 mm x 50 mm x 17 mm, L x W x H). The chosen beam design aims to achieve strength classes C14 and C 10 (definition by [7]) with density graded lamellas for the compression, shear and tension zones. The lamellas of the highest density class are assigned to the tension zone 335...363 kg/m<sup>3</sup> for C 10, respectively >427 kg/m<sup>3</sup> for C 14. Medium density lamellas are in the compression zone

(289...335 kg/m<sup>3</sup> for C 10 respectively 363...427 kg/m<sup>3</sup> for C 14). Low density lamellas are in the shear zone (<289 kg/m<sup>3</sup> for C10 and C14).

For the production of the beams, the two lamella types "natural lamellae" (specimen identification N, cut according to geometry from wider boards and therefore show high density and property gradients) and "assembled lamellas" (specimen identification A, edge-glued of narrow, density graded strips and therefore show more homogeneous density and properties over the width) are used.

#### 3.3 DENSIFIED MATERIAL

To investigate the influence of the densification of lamellas on the GLT properties, material properties of densified oil palm wood are used as input parameters for tension lamellas (only in FEM modelling, no laboratory test). The material is mechanically dewatered and thermo-hydro-mechanically densified using two densification rates (40 % and 60 %). Further information on the process and elastomechanical properties are given in Fruehwald-Koenig et al. [22] and Koelli and Fruehwald-Koenig [23].

#### 3.4 ELASTIC MATERIAL PARAMETERS

Modelling is carried out using two sets of material constants from ultrasonic testing and static testing. The Young's moduli and shear moduli are taken from Fruehwald-Koenig and Faust [16], who described them related on density from ultrasonic tests. Equations (1) - (3) provide the relationships for the Young's moduli and (4) - (6) for the shear moduli [15].

$$E_L(\rho) = 22.345 \rho + 204.89 \quad (1)$$

$$E_R(\rho) = 0.318 \rho + 223.38 \quad (2)$$

$$E_T(\rho) = 1.37 \rho - 42.164 \quad (3)$$

$$G_{RT}(\rho) = 0.6917 \rho - 16.657 \quad (4)$$

$$G_{TL}(\rho) = 1.3857 \rho - 91.621 \quad (5)$$

$$G_{LR}(\rho) = 1.0738 \rho - 37.963 \quad (6)$$

where  $E_{L,R,T}$  = Young's moduli along the anatomical axes (ultrasonic test),  $G_{RT,TL,LR}$  = Shear moduli in symmetry planes (ultrasonic test),  $\rho$  = density  
Equation (7) provides the relationship between Young's modulus in longitudinal direction and density from static test [14].

$$E_{t,0}(\rho) = 0.0021 \rho^{2.41} \quad (7)$$

where  $E_{t,0}$  = Young's modulus longitudinal (static test),  $\rho$  = density.  
Equation (8) shows the relationship between shear modulus in the longitudinal direction and density from static test [16].

$$G_{RL,stat}(\rho) = 0.2812 \rho - 1.7586 \quad (8)$$

where  $G_{RL,static}$  = Shear modulus TL-plane (static test),  $\rho$  = density.

Due to limited data on static tests, the dynamically determined elastic constants are converted in “reduced” (static) properties using the Equations (9) and (10).

$$E_{R,T \text{ reduced}}(\rho) = \left( \frac{E_L(\rho)}{E_{t,0}(\rho)} \right) E_{R,T}(\rho) \quad (9)$$

$$G_{RT,LR \text{ reduced}}(\rho) = \left( \frac{G_{TL}(\rho)}{G_{RL,stat}(\rho)} \right) G_{RT,LR}(\rho) \quad (10)$$

where  $E_{R,T, \text{reduced}}$  = reduced Young’s moduli along R and T axis,  $E_{L,R,T}$  = Young’s moduli along the anatomical axes (ultrasonic test) (Equations (1) – (3)),  $E_{t,0}$  = Young’s modulus longitudinal (static test) (Equation (7)),  $G_{RT,LR, \text{reduced}}$  = reduced shear moduli in RT, LR plane,  $G_{RT,TL,LR}$  = Shear moduli in symmetry planes (ultrasonic test) (Equations (4) – (6)),  $G_{RL,static}$  = Shear modulus TL-plane (static test) (Equation (8)),  $\rho$  = density.

According to Fruehwald-Koenig et al. [17], Poisson’s ratios are not density dependent. Therefore, the mean values  $\mu_{LT} = 0.497$ ,  $\mu_{LR} = 0.497$  and  $\mu_{RT} = 0.117$  are used. For the densified lamellas, the E- and G-values given in Table 1 are used. They are determined using Equations stated in Koelli and Fruehwald-Koenig [23] estimating a density of 550 kg/m<sup>3</sup> and adjustments as described above. As Poisson’s ratios, the ratios for undensified material as stated above are used.

**Table 1:** Material parameters densified tension lamellas

|      | $E_L$<br>[MPa] | $E_R$<br>[MPa] | $E_T$<br>[MPa] | $G_{RT}$<br>[MPa] | $G_{LT}$<br>[MPa] | $G_{LR}$<br>[MPa] |
|------|----------------|----------------|----------------|-------------------|-------------------|-------------------|
| 40 % | 6301.4         | 212.3          | 125.4          | 43                | 139.6             | 148.6             |
| 60 % | 3741.3         | 211.6          | 36.7           | 43                | 139.6             | 157.5             |

### 3.5 PLASTIC MATERIAL PARAMETERS

The compressive yield strength is defined as the strength of a material at the transition from elastic to plastic material behaviour. The determination of the compressive yield strength is realised using [4] and [24] and based on the stress-strain diagrams of the compression tests of oil palm wood in service dimensions carried out by Heister and Fruehwald-Koenig [25].

Starting the determination, a straight line is formed through the linear area of the stress-strain diagram. Subsequent this line is shifted parallel by a plastic strain of 0.02 %. The intersection of the shifted line and the test curve defines the elastic limit. The stress in the intersection point corresponds to the compressive yield strength.

The compressive yield strength longitudinal (L) ranges from 5.3 to 34 MPa (mean 15 MPa). An exponential relationship with density is observed ( $R^2 = 0.76$ , see Equation (11)).

$$f_{c,L}(\rho) = 1.6115 e^{0.0052\rho} \quad (11)$$

where  $f_{c,L}$  = compressive Yield-strength longitudinal,  $\rho$  = density.

The compressive yield strength radial/tangential (R/T) ranges from 0.42 to 0.60 MPa. No relationship with density ( $R^2 = 0.08$ ) can be proven. The mean value of 0.499 MPa is used as input parameter.

Due to the brittle material behaviour of oil palm wood under tensile load, the tensile yield strength is assumed to be equal to the tensile strength. Equation (12) and (13) show the relationship between density and tensile strength (L)  $f_{t,L}$  and tensile strength (R/T)  $f_{t,RT}$  [14].

$$f_{t,L}(\rho) = 0.00004 \rho^{2.12} \quad (12)$$

$$f_{t,RT}(\rho) = 0.0002 \rho^{1.4} \quad (13)$$

where  $f_{t,L}$  = tensile strength (longitudinal),  $f_{t,RT}$  = tensile strength (radial / tangential),  $\rho$  = density.

Due to limited data on the plastic behaviour of oil palm wood under shear stress, shear yield strengths are assumed to be equal to shear strengths.

Equations (14) and (15) show relationships between density and rolling shear strength and shear strength in the R/T plane (longitudinal loading) [14].

$$f_{v,RT}(\rho) = 0,001 \rho^{1.0539} \quad (14)$$

$$f_{v,RL}(\rho) = 0,0004 \rho^{1.3573} \quad (15)$$

where  $f_{v,RT}$  = rolling shear strength,  $f_{v,RL}$  = shear strength (tangential plane, longitudinal load),  $\rho$  = density.

For shear strengths in the transverse plane, no correlations are available in the literature. To approximate the shear strengths in the transverse plane, ratios of shear strengths in different plane-load combinations of beech wood according to Kollmann [26] are used to adjust the rolling shear strength and shear strength in the radial/tangential plane (L).

The hardening modulus is defined as the slope between the compressive yield strength and the compressive strength. The hardening modulus (L) reaches values of 526 to 3193 MPa (mean value 1486 MPa). An relationship with density is observed ( $R^2 = 0.50$ , see Equation (16)).

$$E_{p,L}(\rho) = 254.14 e^{0.004\rho} \quad (16)$$

where  $E_{p,L}$  = hardening modulus (L),  $\rho$  = density.

The hardening modulus (R/T) reaches values from 33.79 to 47.61 MPa. No relationship with density ( $R^2 = 0.00$ ) can be proven. The mean value of the hardening modulus (R/T) (41.86 MPa) is used as input parameter.

## 4 METHODS

### 4.1 DETERMINATION OF FLEXURAL PROPERTIES

The flexural properties of glued laminated timber are determined in accordance with [4] using a four-point bending test. The support points are spaced 18 times the height of the beam ( $h$ ) corresponding to 1836 mm. Load application points are required to be spaced 6  $h$  (612 mm) apart. In the laboratory tests [7] partially deviating distances of 646 mm, 612 mm and 595 mm are used. Deviating from the requirements of the aforementioned standard solid wood (pine, oil palm) and plywood (beech, birch) riders instead of steel are used [7]. Local and global MOE as well as flexural strength are determined according to [4].

### 4.2 DETERMINATION OF MODELLING PARAMETERS AND EXPERIMENTS

The effects of varying parameters on the results of the modelling of GLT beams are investigated. The effects are tested in three experiment sets. In the first experiment set (I), the influences of the parameters geometry (2D / 3D), material model (isotropic, orthotropic), material parameter determination (non-destructive, destructive) implementation of riders and element size (8.5 mm, 5.66 mm) on the elastic flexural properties are investigated. Between each experiment one parameter is changed at a time, this enables the observation of the parameter effect. In each individual experiment, 23 beams are investigated and six experiments are carried out. In the second experiment set (II), the general suitability of FEM for determining the flexural strength of oil palm-based GLT is investigated. Furthermore, the influence of the implementation of riders is again investigated. In addition, densified tension lamellas (cf. section 3.3) are examined separately in two individual experiments. Four different experiments are carried out on 22 GLT beams. In the third experiment set (III), the influence of variations in the material parameters hardening moduli ( $E_{p,L}$ ,  $E_{p,R}$ ,  $E_{p,T}$ ), compressive yield strengths (R/T) ( $f_{c,R}$ ,  $f_{c,T}$ ), material model (orthotropic plastic: compression zone / total specimen), tensile yield strength (L) ( $f_{t,L}$ ) and shear yield strengths ( $f_{v,RT}$ ,  $f_{v,LT}$ ,  $f_{v,LR}$ ) are investigated on a homogeneous beam model with lamellas of the same density. The total sum of the individual experiments of the third experiment set is 17.

### 4.3 EXPERIMENT IMPLEMENTATION IN MODELLING SOFTWARE

The modelling is realised using RFEM 6.02 (Dlubal Software GmbH). The beams are represented as two- or three-dimensional geometric models. The lamellas are represented by planes or volume elements. A solid bond is assumed between the lamellas. Modelling of the adhesive joints is omitted in this work, as no failure of the adhesive joints is reported in the laboratory tests. Isotropic linear and orthotropic linear elastic material models are used to model the local and global MOE. For modelling the flexural strength orthotropic plastic material behaviour is assigned to the compression zone,

tension and shear zone are described by orthotropic linear elastic material behaviour. For the description of the material behaviour, nine (orthotropic linear elastic) respectively 21 (orthotropic plastic) material parameters are necessary. The material parameters are determined as described in sections 3.4 and 3.5.

The support is realised as nodal supports or line supports. Displacements along the Y- and Z-axes are omitted. Along the X-axis displacements are possible. The bearings in the X-direction are described by a spring ( $k = 0.1$  kN/m).

The lamellas are modelled with the help of two- and three-dimensional, rectangular plate or cubic volume elements. The element size is set to 5.66 mm or 8.5 mm, which corresponds to two respectively three elements over the height of one lamella. Depending on the settings the models are formed out of 3108 – 366019 elements with 3380 - 110802 nodes.

Loads are applied as nodal or line loads. Half of the total load is applied at each of the two load application points. For the determination of the elastic flexural properties, the loads are applied in two steps representing 10 % and 40 % of the estimated maximum load. The application of the orthotropic plastic material model requires stepwise calculations. Within each load step, equilibrium is determined using the Newton-Raphson method with a maximum of 100 iterations. The load is increased in steps of 50 N as a compromise between accuracy and calculation time.

Four nodal supports are used to determine the deflection necessary to calculate the elastic flexural properties. The supports are arranged according to [4]. To determine the maximum load required to calculate the flexural strength, the longitudinal stresses at raster points on the tensile lamellas are compared to the tensile strength of the corresponding lamella. Failure occurs when the recorded stress exceeds the tensile strength. Tensile strengths and stresses are compared at each load level. Load and stress of the failure load level and the previous load level are used to determine the maximum load by interpolation.

The deformation and stresses are calculated using the solver implemented in RFEM 6.02 and according to first-order theory. The results are presented in the form of graphical representations of the result gradients and tabular output of results in nodes and at grid points (10 mm spacing, total 7120 grid points) on the boundary surfaces of the tension lamellas.

## 5 RESULTS AND DISCUSSION

### 5.1 RESULTS FOR LOCAL MOE

Table 2 shows statistical variation parameters of the first experiment set regarding the local MOE. The mean values reach from 4050 MPa to 9625 MPa (laboratory tests 5422 MPa).

Normal distribution can be assumed for all experiments and laboratory tests acc. to an Anderson-Darling test. A one-factor ANOVA and a posterior pairwise t-test with alpha error correction according to Bonferroni shows significant differences of the mean values.

**Table 2:** Statistical variation parameters local MOE

|                     | Parameter              | Min [MPa] | Max [MPa] | Mean [MPa] | Sd [MPa] | COV [%] |
|---------------------|------------------------|-----------|-----------|------------|----------|---------|
| Exp. I.1            | 2D, iso, nr, nd, 8.5   | 7934      | 10848     | 9347       | 838      | 8.97    |
| Exp. I.2            | 3D, iso, nr, nd, 8.5   | 8238      | 11078     | 9625       | 832      | 8.64    |
| Exp. I.3            | 3D, ortho, nr, nd, 8.5 | 7961      | 10701     | 9313       | 815      | 8.75    |
| Exp. I.4            | 3D, ortho, nr, d, 8.5  | 2759      | 5768      | 4155       | 864      | 20.78   |
| Exp. I.5            | 3D, ortho, r, d, 8.5   | 2756      | 5613      | 4051       | 820      | 20.23   |
| Exp. I.6            | 3D, ortho, r, d, 5.66  | 2746      | 5603      | 4050       | 823      | 20.32   |
| laboratory test [7] |                        | 3151      | 7128      | 5422       | 1055     | 19.46   |

2D/3D: model dimension, iso/ortho: iso-/orthotropic, r/n.r.: rider, no rider, d./n.d: destructive, non-destructive material parameter, 5.66/8.5: element size

Figure 1 shows the relationships between density and local MOE (experiments and laboratory test). The results of the local MOE show linear correlations with the density in all individual experiments with  $R^2$  between 0.52 and 0.55. The slopes of the linear relationships are lower than that of the laboratory test. Differences between the equations of the regression lines are limited to the ordinate intercept. The regression lines are parallel shifted.

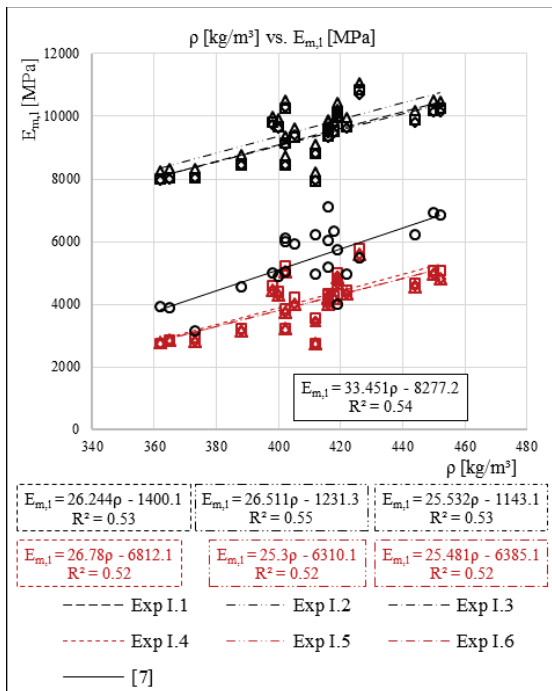


**Figure 1:** Relationship between density and local MOE (statistical variation parameters see Table 2)

## 5.2 RESULTS FOR GLOBAL MOE

Table 2 shows statistical variation parameters of the first experiment set regarding the global MOE. The mean values reach from 7447 MPa to 18513 MPa (laboratory tests 4562 MPa). Normal distribution can be assumed for all experiments and laboratory tests acc. to an Anderson-Darling test.

A one-factor ANOVA and a posterior pairwise t-test with alpha error correction according to Bonferroni shows significant differences of the mean values.

**Table 3:** Statistical variation parameters global MOE

|                     | Parameter              | Min [MPa] | Max [MPa] | Mean [MPa] | Sd [MPa] | COV [%] |
|---------------------|------------------------|-----------|-----------|------------|----------|---------|
| Exp. I.1            | 2D, iso, nr, nd, 8.5   | 15806     | 21414     | 18513      | 1666     | 9.00    |
| Exp. I.2            | 3D, iso, nr, nd, 8.5   | 15475     | 20500     | 18053      | 1544     | 8.55    |
| Exp. I.3            | 3D, ortho, nr, nd, 8.5 | 14955     | 19911     | 17501      | 1515     | 8.66    |
| Exp. I.4            | 3D, ortho, nr, d, 8.5  | 5092      | 9953      | 7447       | 1442     | 19.37   |
| Exp. I.5            | 3D, ortho, r, d, 8.5   | 5128      | 10350     | 7773       | 1562     | 20.10   |
| Exp. I.6            | 3D, ortho, r, d, 5.66  | 5128      | 10335     | 7779       | 1544     | 19.85   |
| laboratory test [7] |                        | 2541      | 6142      | 4562       | 1022     | 22.41   |

2D/3D: model dimension, iso/ortho: iso-/orthotropic, r/n.r.: rider, no rider, d./n.d: destructive, non-destructive material parameter, 5.66/8.5: element size

Figure 2 shows the relationships between density and global MOE (experiments and laboratory test). The results of the global MOE show linear correlations with the density in all individual experiments with  $R^2$  between 0.53 and 0.57. The slopes of the linear relationships are higher than that of the laboratory test differences between the equations of the regression lines are limited to the ordinate intercept. The regression lines are parallel shifted.

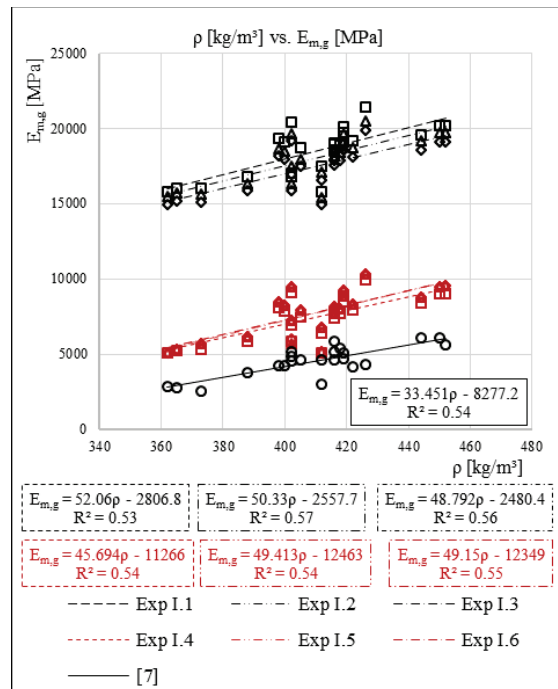


**Figure 2:** Relationship between density and global MOE (statistical variation parameters see Table 3)

### 5.3 DISCUSSION LOCAL AND GLOBAL MOE

The differences between the experiments can be attributed to varying factors. The difference between experiment I.1 and I.2 is the geometrical dimension (2D, 3D). Only minor effects for components homogeneous across the width occur. The small difference between experiment I.2 and I.3 after changing the material model is attributed to the load case. In four-point bending tests, stresses primarily occur in fibre direction. According to Ehlbeck et al. [18], the Young's modulus in the fibre direction is the dominating factor for the flexural properties of GLT beams. The Young's modulus in fibre direction is not varied between experiment I.2 and I.3. The implementation of riders according to [4] in experiments I.5 and I.6 shows no significant effect. The modelling is carried out in the elastic range of the material behaviour of the oil palm wood (no plastic deformations occur). The riders serve to distribute and transmit the load. Minimising the element size (experiment I.6) shows no significant effect in this study. Discretisation by using two or three elements over the lamella thickness is considered sufficient [28]. The significant differences between experiment groups I.1 – I.3 and I.4 – I.6 are attributed to the choice of material parameters. The difference of the Young's modulus in the fibre direction as one of the main influencing parameters corresponds to 55.4 %. The differences for local MOE (56.7 %) and global MOE (57.5 %) between the experiment groups show similar percentages.

Comparison of the local and global MOE shows that the global MOE exceeds the local MOE in all experiments. Heister and Fruehwald-Koenig [7] report an opposite relationship for the laboratory tests (local MOE > global MOE). The ratio of the mean values of local to global MOE ranges from 0.505 to 0.558. The laboratory tests provide a ratio of 1.189 (0.99 spruce [29]). Thus, the modelled values are below the comparative literature values. Boström [30] reports for spruce, that the local MOE > global MOE if the global MOE is > 10 GPa and local MOE < global MOE if the global is < 10 GPa. Boström [29] attributes the differences between local and global MOE to shear deformations and the influence of timber defects in small cross-sections. The effects described are consistent with the results of experiments I.4 – I.6. Applying one density the whole lamella, leads to a reduction of the natural property gradients (artificial homogenisation). The absence of these natural property variations and defects results in comparably higher values for the global MOE, the influence on the local MOE is less pronounced.

### 5.4 RESULTS FOR FLEXURAL STRENGTH

Table 4 shows statistical variation parameters of the second experiment set regarding the flexural strength. The mean values are 13.3 MPa and 13.9 MPa (laboratory tests 22.1 MPa). Normal distribution cannot be proven for all experiments. Only the laboratory test shows normal distribution according to an Anderson-Darling test. A Friedman-Test and a posterior pairwise, paired Wilcoxon-Test with alpha error correction according to Bonferroni

shows significant differences between the experiments and the laboratory test.

**Table 4:** Statistical variation parameters flexural strength

|                     | Parameter | Min [MPa] | Max [MPa] | Mean [MPa] | Sd [MPa] | COV [%] |
|---------------------|-----------|-----------|-----------|------------|----------|---------|
| Exp. II.1           | nr        | 9.5       | 15.7      | 13.3       | 2.2      | 16.5    |
| Exp. II.2           | r         | 9.7       | 16.5      | 13.9       | 2.4      | 17.5    |
| laboratory test [7] |           | 11.7      | 29.7      | 22.14      | 5.57     | 25.16   |

r/n.r.: rider, no rider

Figure 3 shows the relationships between density and flexural strength divided for specimen groups A (assembled) and N (natural).  $R^2$  ranges from 0.53 to 0.55. The slope of the laboratory test is steeper than the experimental slopes for specimen group N. The regression lines of the laboratory results from Heister and Fruehwald-Koenig [7] lie above the regression lines of the experiments. Specimen group A (assembled) shows similar slopes for experiments and laboratory tests. The regression lines of specimen group N (natural) agree for the experiments, but differ to that from laboratory testing. This leads to the conclusion, that inhomogeneity and variations in material properties influence the results of the flexural test. Further tests are recommended to enable reliable statements about the stochastic behaviour of the flexural properties of oil palm based GLT.

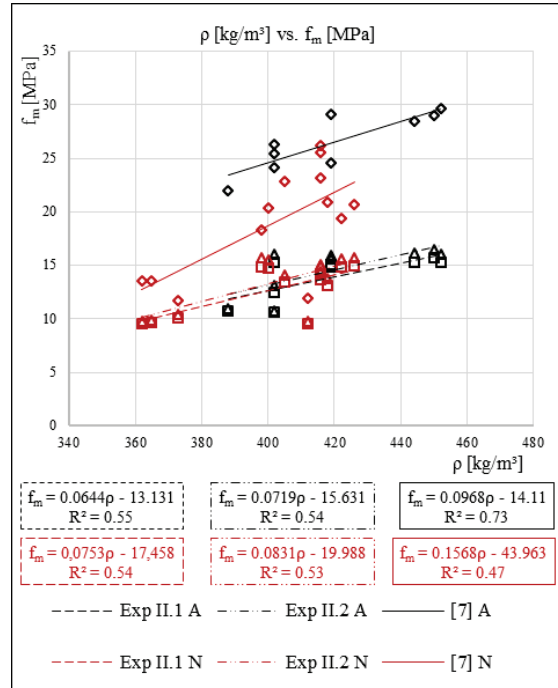


**Figure 3:** Relationship between density and flexural strength divided by specimen group A (assembled) and N (natural)

The comparison with the results of Heister and Fruehwald-Koenig [7] shows mean percentage deviations of -38.6 %. These deviations tend to correspond to the deviations of the local MOE (-25.5 %). Increasing the values of the elastic constants leads to stiffer material behaviour. This in turn results in loads being transferred with a certain delay and thus the critical tensile strengths in the tensile zone are reached later. The flexural strength increases. Further, the choice of the material model influences the flexural strength. Blaß et al. [19] point out that the use of the linear elastic material model in the tensile zone leads to an underestimation of the flexural strength. Plastic material behaviour in the tensile zone results in stress redistributions and thus a delayed attainment of the critical tensile stress. The sensitivity analysis (see section 5.8) shows that the application of the orthotropic plastic material model in the tensile zone results in an increase of the flexural strength of about 3.8 %.

Figure 4 shows the relationships between the density of the tensile lamellas and the flexural strength. Linear relationships are observed ( $R^2 = 0.83$  Exp. II.1,  $R^2 = 0.84$  Exp. II.2).  $R^2$  (0.39) for the laboratory is lower compared to the experiments. Deviation from the behaviour observed for specimen group N (natural) in Figure 3, the regression line of the data from Heister and Fruehwald-Koenig [7] runs roughly parallel above the regression lines of the experiments. It can be observed that the density of the tension lamellas shows better correlations to the flexural strength than the overall density of the GLT beams.

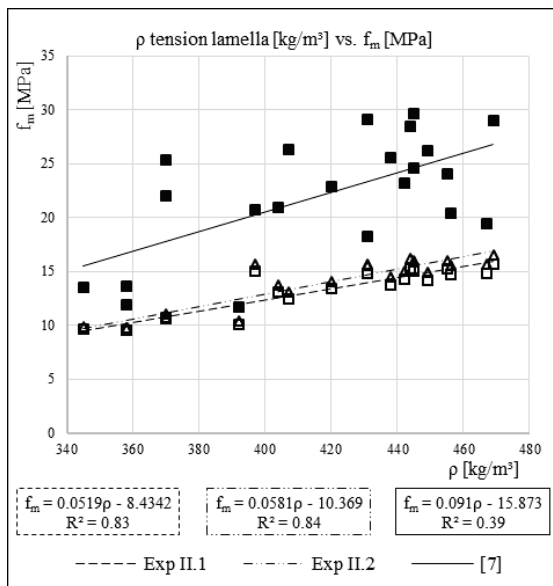


**Figure 4:** Relationship between density tension lamella and flexural strength

The differences between experiment II.1 and experiment II.2 are due to the change in the supports and load application points. Two effects can be observed due to the introduction of riders. The first effect is that plastic deformations are initiated later due to the load distribution over a larger area. Frese [20] confirms this effect by

modelling homogeneous comparison beams. The second effect is the change in the stress profile within the tension lamella. As described by Frese [20], a rounding of the stress profile can be observed, which leads to the critical tensile stress being reached later. The mean percentage deviation between the experiments of 4.6 % exceeds the value of 1 % reported by Frese [20] for beech. The effect of load distribution by the riders therefore is higher for oil palm wood. The observed behaviour might be explained by the comparably low compressive strength (R/T) of oil palm wood.

## 5.5 INFLUENCE OF DENIFIED TENSION LAMELLAS

The use of tension lamellas of uniform density ( $550 \text{ kg/m}^3$ ) in all test specimens results in a reduction of the observed variations. These variations represent the influence of the remaining test specimen structure. The flexural strength is increased compared to the comparison experiment (Exp. II.2) up to a density of  $398 \text{ kg/m}^3$  (40 % dens.) and  $434 \text{ kg/m}^3$  (60 % dens.). Surpassing those aforementioned thresholds, the flexural strength is decreased. This reflects the results of Koelli and Fruehwald-Koenig [23], who report that at the same density, undensified specimens show higher flexural strengths than densified specimens. This explains why despite the higher density of the densified tensile lamellas ( $550 \text{ kg/m}^3$ ), no improvement in flexural strength can be achieved when the thresholds are exceeded. Densified tension lamellas are therefore particularly suitable for improving the flexural properties of low-density beam structures.

## 5.6 SENSITIVITY ANALYSIS

Within the sensitivity analysis, influences of the factors listed in section 4.2 on the flexural strength are investigated on the basis of percentage deviations from the comparison experiments III.C1 and III.C2 (Table 5). Reducing the hardening modulus (R/T) from 41.9 MPa to 4.4 MPa in experiment III.1.1 reduces the flexural strength to 12.0 MPa (-3.6 %). A further reduction of the hardening modulus (R/T) to 0.2 MPa in experiment II.1.2 results in a further reduction of the flexural strength to 10.8 MPa (-13.7 %).

Variation of the compressive yield strength (R/T) shows little influence on the modelling results. Increasing the compressive yield strength (R/T) to 1 MPa (100 % increase) in experiment III.2.1 results in an increase in flexural strength of 0.005 MPa (+0.03 %). Increasing the compressive yield strength (R/T) to 4 MPa (700 % increase) in experiment III.2.2 results in an increase in flexural strength of 0.1 MPa (+0.3 %).

In experiment III.C2, the orthotropic plastic material model is assigned to all lamellas of the comparative specimen. Due to this change, the flexural strength of the reference specimen is increased to 13.0 MPa (+3.8 %). The change of the material model, reduces the compressive stresses in the support area. As described by Blaß et al. [19], stress redistributions in the tensile zone are possible using orthotropic plastic material behaviour, which lead to the critical tensile stress being reached later.

Experiments III.3 and III.4 evaluate the effects of a combination of the change of the material model and increased tensile yield strength (L). When changing the tensile yield strength (L), two separate considerations are to be carried out depending on the chosen comparative tensile strength (L) of the tensile lamellas (cf. section 4.3). Not increasing the critical tensile strength (L) and keeping it at 13.1 MPa (Exp. III.3.2 and III.4.2), results in flexural strengths of 13.0 MPa (-0.1 %, Exp. III.3.2 and Exp. III.4.2). Increasing the critical tensile strength (L) according to the increased tensile yield strength (L), results in flexural strengths of 19.6 MPa (+50.9 %, Exp. III.3.1) and 28.9 MPa (+123.3 %, Exp. III.4.1). The recorded percentage increases of flexural strengths are equal to the percentage increases of the applied tensile yield strengths (L) of 52.32 % and 128.48 %.

The increase of the shear yield strengths (Exp. III.5) shows only little influence on the flexural strength of the comparative specimen, (increase of 0.02 %) because of the choice of test arrangement. In four-point bending tests, only low shear stresses occur.

The sensitivity analysis shows that variations in the hardening moduli have a large influence on the flexural bending strength and needs further investigations. Variations of tensile yield strengths (L) with simultaneous adjustment of the critical tensile strength shows strong effects and needs further investigations. Variations in compressive yield strength and shear yield strength have small influence on the flexural strength. The parameters are applicable in the chosen form.

**Table 5:** Sensitivity analysis result and percentage deviations

|                | III.C1 | III.1.1 | III.1.2 | III.2.1 | III.2.2 |       |
|----------------|--------|---------|---------|---------|---------|-------|
| $f_m$<br>[MPa] | 12.5   | 12.0    | 10.8    | 12.5    | 12.5    |       |
| Deviation [%]  |        | 3.6     | 13.7    | 0.03    | 0.3     |       |
|                | III.C2 | III.3.1 | III.3.2 | III.4.1 | III.4.2 | III.5 |
| $f_m$<br>[MPa] | 13.0   | 19.6    | 13.0    | 28.9    | 13.0    | 13.0  |
| Deviation [%]  |        | 50.9    | 0.06    | 123.3   | 0.07    | 0.04  |

Exp. III.1: reduction hardening moduli (R/T), Exp. III.2: increase compressive yield strength, Exp. III.3: change material model, increase tensile yield strength (L), Exp. III.4: change material model, increase tensile yield strength (L), Exp. III.5: change material model, increase shear yield strength

## 6 CONCLUSION AND OUTLOOK

The results of the modelling confirm the applicability of the finite element method for modelling oil palm wood-based GLT. The selected geometric models as volume and plane models based on individual layers with varying material properties as well as the chosen support and load application implementation are suitable for a realistic representation of the comparative tests.

Geometric representation, material model, riders as well as element size show no significant influence on the results of the modelling of the local and global MOE, whereas the material parameter determination has a significant influence on the modelled MOE. Deviating from this, the implementation of riders shows a significant influence on the modelling results of the flexural strength.

In further investigations, an implementation of riders is strongly recommended.

The comparison of the flexural properties (MOE and flexural strength) with the results of the laboratory tests by Heister and Fruehwald-Koenig [7] shows significant differences due to the material constants used (elastic constants and tensile strength) and the material model used in the tensile zone. The effects of material constants and material model adjustments have to be investigated in experiments on a larger scale.

The relationships between density and local and global MOE proven in this work show comparable forms to Heister and Fruehwald-Koenig [7], whose differences lie primarily in the ordinate intercepts determined. Comparable behaviour is shown by the relationships between density of the specimens and flexural strength (for specimen group A (assembled lamella)) and between tensile lamella density and flexural strength (overall collective). The overall collective as well as specimen group N (natural lamella) show uniform shapes within the modelling for the relationship between density and flexural strength but deviate strongly from the results of Heister and Fruehwald-Koenig [7]. An adjustment of the ordinate intercept is not expedient. The observed behaviour offers a starting point for further investigations regarding the optimisation of the modelling results. The use of densified tension lamellas results in a homogenisation of the flexural strength. Especially the performance of lower density specimens can be improved by using densified tension lamellas. The level of improvement is higher for higher densification rates.

The local and global MOE of the modelling show a different behaviour compared to the literature. The global MOE exceeds the local MOE in all experiments. Further investigations on the global MOE are recommended. An effect of the artificial homogenisation, by applying only one density for one lamella and reducing the natural property gradients, on the results of the global MOE can be demonstrated for specimen group N (natural).

The sensitivity analysis identifies the hardening modulus, the tensile yield strength (L) and the choice of material model in the tensile zone as parameters that strongly influence the results of the flexural strength. The parameters compressive yield strength (R/T) and shear yield strength show much lower influence. The sensitivity analysis is suitable for determining parameter influences. The results of this work offer starting points for further investigations, in particular the consideration of the influencing factors identified in this work, the modelling of oil palm-based cross laminated timber as well as the application of statistically varying material constants for the representation of larger specimen collectives and the improved representation of natural property variations within the lamellas.

## ACKNOWLEDGEMENTS

The laboratory tests referred to in this study were carried out by Prof.'in Dipl.-Holzwirtin Katja Fruehwald-Koenig (creation of a grading system for oil palms, lamella grading and determination of the GLT structure) and Lena Heister M.Sc. (production and testing of the GLT beams).

The evaluation and results of the investigations can be found in the publication by Heister and Fruehwald-Koenig [7]. The investigation was financed by the German Federal Ministry of Education and Research through the “Bioökonomie International 2017” project “Oilpalmsugar (031B0767A)”, as well as the Ministry of Culture and Science of the State of North Rhine-Westphalia through the project “005-2105-0054”.

## REFERENCES

- [1] Food and Agriculture Organization of the United Nations: Crops and livestock products. <https://www.fao.org/faostat/en/#data/QCL>, 2023.
- [2] Lim S. C., Khoo K. C.: Characteristics of oil palm trunk and its potential utilization. *Malaysian Forest*, 49:3–22, 1986.
- [3] Fruehwald A., Fruehwald-Koenig K.: The Use of Oil Palm Trunks for Wood Products. In: *By-Products of Palm Trees and Their Applications*, 69–80, 2019
- [4] EN 408+A1:2012-07: Timber structures - Structural timber and glued laminated timber - Determination of some physical and mechanical properties. CEN European Committee for Standardization, 2012.
- [5] EN 14080:2013-06: Timber structures - Glued laminated timber and glued solid timber - Requirements. CEN European Committee for Standardization, 2013.
- [6] Fruehwald-Koenig K.: Properties and Grading of Oil Palm Lumber. In: *Proceedings: 21<sup>st</sup> International Nondestructive Testing and Evaluation of Wood Symposium*, 204–212, 2019
- [7] Heister L., Fruehwald-Koenig K.: Glued Laminated Timber from Oil Palm Timber – Beam Structure, Production and Elastomechanical Properties. In: *Proceedings of 2nd World Conference on Byproducts of Palms and Their Applications*, 29–44, 2022.
- [8] Tomlinson P. B., Horn J. W. and Fisher J. B.: *The anatomy of palms: Arecaceae - Palmae*. Oxford University Press, 2011.
- [9] E. S. Bakar, M. H. Sahri, and P. S. H'ng. Anatomical characteristics and utilization of oil palm wood. In T. Nobuchi, M. H. Sahri, *The formation of wood in tropical forest trees—a challenge from the perspective of functional wood anatomy*, pages 161–178. Penerbit Universiti Putra, Malaysia, 2008.
- [10] Killmann W., Lim S. C.: Anatomy and properties of oil palm stem. In: *Proceedings National Symposium of Oil Palm By-Products*, 1–25, 1985.
- [11] Koelli N.: Density and Moisture Distribution in Oil Palm Trunks from Peninsular Malaysia. Bachelor-Thesis, University of Hamburg, Hamburg, 2016.
- [12] Fathi L.: Structural and mechanical properties of the wood from coconut palms, oil palms and date palms. PhD-Thesis, University of Hamburg, Hamburg, 2014.
- [13] Srivaro S., Matan N., Lam F.: Property gradients in oil palm trunk (*Elaeis guineensis*). *Journal of Wood Science*, 64(6):709–719, 2018.
- [14] Fruehwald-Koenig K., Heister L.: Macro- and Micromechanical Behavior of Oil Palm Wood (*Elaeis guineensis* JACQ.): Tensile, Compression and Bending Properties. Submitted publication, 2023.
- [15] Fruehwald-Koenig K., Faust B.: Evaluation of Elastic Constants of Oil Palm Wood using Ultrasonic Measurement. In: *Proceedings: 22<sup>st</sup> International Nondestructive Testing and Evaluation of Wood Symposium*, 29–39, 2022.
- [16] Koelli N.: Relation shear modulus and density for oil palm wood (*Elaeis guineensis* JACQ.). Personal communication, 2022.
- [17] Fruehwald-Koenig K., Faust B., Hackel M.: Macromechanical and Micromechanical Behavior of Oil Palm Wood (*Elaeis guineensis* JACQ.): Elastic Constants and Shear Strength. Publication in preparation, 2023.
- [18] Ehlbeck J., Colling F., Görlacher R.: Einfluß keilgezinkter Lamellen auf die Biegefestigkeit von Brettschichtholzträgern. *Holz als Roh- und Werkstoff*. 43(8):333–337, 1985.
- [19] Blaß H. J., Denzler J., Frese M., Glos P. and Linsemann P.: Biegefestigkeit von Brettschichtholz aus Buche. *Universitätsverlag Karlsruhe*, 2006.
- [20] Frese M.: Die Biegefestigkeit von Brettschichtholz aus Buche. Experimentelle und numerische Untersuchungen zum Laminierungseffekt. *Universitätsverlag Karlsruhe*, 2006.
- [21] Gao Y., Wu Y., Zhu X., Zhu L., Yu Z., Wu Y.: Numerical Analysis of the Bending Properties of Cathay Poplar Glulam. *Materials* 8(10):7059–7073, 2015
- [22] Fruehwald-Koenig K., Koelli N., Fruehwald A.: Mechanical Dewatering of Wet Oil Palm Lumber Prior to Press-Drying. In: *Proceedings of 2nd World Conference on Byproducts of Palms and Their Applications*, 11–27, 2022.
- [23] Koelli N., Fruehwald-Koenig K.: Elastomechanical Properties of Thermo-Hygro-Mechanical (THM) Densified Oil Palm Lumber. Submitted publication, 2023.
- [5] DIN 50099:2018-12: Tensile testing of metallic cellular materials. DIN Deutsches Institut für Normung e. V., 2018.
- [25] Heister L., Fruehwald-Koenig K.: Compression and Tensile Properties Oil Palm Wood (*Elaeis guineensis* JACQ.) Specimen in Dimension of Use. Submitted publication, 2023b.
- [26] Kollmann F.: *Technologie des Holzes und der Holzwerkstoffe: Anatomie und Pathologie, Chemie, Physik, Elastizität und Festigkeit*. 2nd ed. Springer Berlin Heidelberg, 1951.
- [27] Vida C., Lukacevic M., Eberhardsteiner J., Füssl J.: Modeling approach to estimate the bending strength and failure mechanisms of glued laminated timber beams. *Engineering Structures*, 255:113862, 2022.
- [28] Boström L.: Determination of the modulus of elasticity in bending of structural timber - comparison of two methods. *Holz als Roh- und Werkstoff*, 57(2):145–149, 1999.